

$^{12}\text{C} + ^{12}\text{C} \rightarrow ^8\text{Be}_{\text{g.s.}} + ^{16}\text{O}_{\text{g.s.}}$  resonance reaction around  $E_{\text{c.m.}} = 32.5$  MeV

 M. Takashina,<sup>1,\*</sup> M. Ito,<sup>2</sup> Y. Kudo,<sup>1</sup> S. Okabe,<sup>3</sup> and Y. Sakuragi<sup>1</sup>
<sup>1</sup>*Department of Physics, Osaka City University, Osaka 558-8585, Japan*
<sup>2</sup>*Division of Physics, Graduate School of Science, Hokkaido University, Sapporo 060-0810, Japan*
<sup>3</sup>*Center for Information and Multimedia Studies, Hokkaido University, Sapporo 060-0811, Japan*

(Received 8 November 2002; published 31 January 2003)

A resonance observed in the excitation function of the  $^{12}\text{C} + ^{12}\text{C} \rightarrow ^8\text{Be}_{\text{g.s.}} + ^{16}\text{O}_{\text{g.s.}}$   $\alpha$ -transfer reaction around  $E_{\text{c.m.}} = 32.5$  MeV is studied by the method of coupled-channel Born approximation (CCBA), in which the distorted waves are given by the microscopic coupled-channel (CC) calculations and the  $\alpha$ -transfer reaction processes are treated as the one-step transitions. The CCBA calculation reproduces well the characteristic behavior of the excitation function as well as the angular distribution at the on-resonance energy. The result of the analysis suggests that the  $(\alpha + \alpha) + (\alpha + ^{12}\text{C})$  type four-cluster states are populated in this reaction.

DOI: 10.1103/PhysRevC.67.014609

PACS number(s): 25.70.Ef, 21.60.Gx, 24.10.Eq, 27.30.+t

One decade ago, an interesting resonancelike structure was discovered [1] in the excitation function of the  $^{12}\text{C} + ^{12}\text{C}$  collision leading to the  $^{12}\text{C}(0_2^+) + ^{12}\text{C}(0_2^+)$  exit channel around  $E_{\text{c.m.}} = 32.5$  MeV. This resonance energy corresponds to a high excitation energy of about 46 MeV with respect to the ground state of  $^{24}\text{Mg}$ . Since the  $0_2^+$  state in  $^{12}\text{C}$  is known to have a well-developed  $3\alpha$ -cluster structure, the observed resonance has been expected to be a multicluster state consisting of six  $\alpha$  particles in highly excited  $^{24}\text{Mg}$  nucleus. Thereafter, in order to further investigate the multicluster structures of  $^{24}\text{Mg}$ , a number of experiments have been performed on the  $^{12}\text{C} + ^{12}\text{C}$  system in the same energy region, and similar resonances have been observed [2–4] in other exit channels, including multicluster ones such as  $^{12}\text{C}_{\text{g.s.}} + ^{12}\text{C}(0_2^+)$  and  $^8\text{Be}_{\text{g.s.}} + ^{16}\text{O}_{\text{g.s.}}$ , which decay into the  $^{12}\text{C} + 3\alpha$  and  $2\alpha + ^{16}\text{O}$  configurations, respectively.

The resonances in the  $^{12}\text{C} + ^{12}\text{C}$  inelastic channels had been analyzed systematically by Hirabayashi *et al.* [5] and Ito *et al.* [6,7] based on the microscopic coupled-channel (CC) method. Their calculation reproduced well the observed excitation functions of the various inelastic channels, and they concluded that the resonances in the  $^{12}\text{C}(0_2^+) + ^{12}\text{C}(0_2^+)$  and  $^{12}\text{C}_{\text{g.s.}} + ^{12}\text{C}(0_2^+)$  channels have weakly coupled two  $3\alpha$  and  $^{12}\text{C}$  plus  $3\alpha$  structures, respectively. The successful results in Refs. [5–7] indicate that the microscopic CC is a powerful method to analyze heavy-ion reactions and that it is meaningful to apply this method to analyze the resonance in the  $^8\text{Be}_{\text{g.s.}} + ^{16}\text{O}_{\text{g.s.}}$  exit channel, which is also important to understand the multicluster state in highly excited  $^{24}\text{Mg}$  nucleus.

The aim of this paper is to study the resonance observed in the  $^{12}\text{C} + ^{12}\text{C} \rightarrow ^8\text{Be}_{\text{g.s.}} + ^{16}\text{O}_{\text{g.s.}}$   $\alpha$ -transfer reaction using the microscopic CC method, and to investigate the possibility to understand the resonance at  $E_{\text{c.m.}} = 32.5$  MeV in terms of the multicluster state of  $^{24}\text{Mg}$ .

Since the resonance in the  $\alpha$ -transfer reaction is observed in the same energy region where the resonances in the inelastic channels are observed, one might expect that these reso-

nances were strongly correlated to each other. However, this does not seem to be plausible because the nuclear structure of the exit ( $^8\text{Be}_{\text{g.s.}} + ^{16}\text{O}_{\text{g.s.}}$ ) channel is very different from that of the initial ( $^{12}\text{C} + ^{12}\text{C}$ ) channels and, hence, the  $\alpha$  transfer could take place by a one-step transition. Namely, the direct transition between the entrance and exit channels is expected to be too weak to generate a resonance through the  $\alpha$ -transfer process. It may be more plausible that the resonance observed in the  $\alpha$ -transfer reaction reflects a resonance structure produced either in the initial  $^{12}\text{C} + ^{12}\text{C}$  system or in the final  $^8\text{Be} + ^{16}\text{O}$  system independently, through the resonating distorted waves of one of the systems. Furthermore, the narrow resonance in the  $\alpha$ -transfer reaction, the width of which is  $\sim 1$  MeV, may imply that the resonance is produced only in the final  $^8\text{Be} + ^{16}\text{O}$  system, because there is no such prominent resonance in the inelastic channels in this energy region. Therefore, we first investigate the resonance state of the  $^8\text{Be} + ^{16}\text{O}$  system by the microscopic CC method.

The phenomenological internuclear potential of the  $^8\text{Be} + ^{16}\text{O}$  system cannot be determined because the ground state of  $^8\text{Be}$  is unbound and no elastic scattering data are available. Therefore, we construct the internuclear potential by the double-folding model (DFM) based on the density-dependent  $N-N$  interaction called DDM3Y [8,9]. This model is known to give a reliable shape and strength of the potential between complex nuclei over a wide range of collision energies [8,10].

Since we investigate the resonance structure of the  $^8\text{Be} + ^{16}\text{O}$  system, we perform a microscopic CC calculation including the inelastic channels. In the CC calculation, the diagonal and coupling potentials are given by the DFM:

$$V_{\alpha(ij)\alpha'(k\ell)}(\mathbf{R}) = \int \rho_{ik}^{(a)}(\mathbf{r}_a) \rho_{j\ell}^{(A)}(\mathbf{r}_A) \times v_{NN}(\mathbf{r}_a + \mathbf{R} - \mathbf{r}_A) d\mathbf{r}_a d\mathbf{r}_A, \quad (1)$$

where  $\rho_{ik}^{(a)}$  ( $\rho_{j\ell}^{(A)}$ ) represents the transition density of the projectile (target) nucleus between the state  $i(j)$  in channel  $\alpha$  and the state  $k(\ell)$  in channel  $\alpha'$ , and  $v_{NN}$  is the DDM3Y interaction.

\*Electronic address: takasina@ocunp.hep.osaka-cu.ac.jp

The transition densities of  $^{16}\text{O}$  are given by the  $\alpha + ^{12}\text{C}$  orthogonality-condition-model (OCM) calculation [11], which reproduces well the electron-scattering form factors and electromagnetic transition rates among the ground and excited states of the nucleus. We include the coupling among the ground state ( $0_1^+$ ) and the  $3_1^-$ ,  $0_2^+$ , and  $2_1^+$  excited states. It is well known that the latter two states have an  $\alpha + ^{12}\text{C}$  cluster configuration, while the other two states have a shell-model-like character. The reason why we include these four states in  $^{16}\text{O}$  is following. The coupling between the ground state and the  $3_1^-$  state is important due to the similarity of the nuclear structure of these states. On the other hand, the inelastic transition to the  $0_2^+$  and  $2_1^+$  states from the ground state is expected to be weak compared to that to the  $3_1^-$  state due to the large difference of nuclear structure. However, in the  $\alpha$ -transfer reaction of interest here, the  $\alpha + ^{12}\text{C}$  like cluster states can easily be populated, and hence it is important to investigate the resonance structure in the  $^8\text{Be} + ^{16}\text{O}(0_2^+, 2_1^+)$  channels, although these channels are rather weakly populated in the inelastic transition from the  $^8\text{Be} + ^{16}\text{O}_{\text{g.s.}}$  channel.

For the  $^8\text{Be}$  nucleus, we include the ground state ( $0_1^+$ ) and the  $2_1^+$  and  $4_1^+$  excited states, which form a rotational band, and the couplings among these states are very strong. The transition densities for these states are calculated in terms of the  $2\alpha$  OCM. Since none of the states in  $^8\text{Be}$  are bound states, we discretize the  $\alpha + \alpha$  resonance wave functions by smoothly connecting the resonance wave function to a Gaussian function having a slowly damping tail around the barrier region and then renormalize the wave function with a damped tail. We find that the resultant transition density calculated by the damped wave function is not very sensitive to the choice of the matching radius and the range of the Gaussian function to be connected. Since no scattering data are available for the  $^8\text{Be} + ^{16}\text{O}$  system, we switch off the imaginary potential to avoid the ambiguity due to the choice of the imaginary-potential parameters.

To see the resonance behavior of the system clearly, we define the quantity  $I$  as

$$I = \sum_{\alpha'} \int_0^{R_{\max}} dR |\chi_{\alpha'}^{(\alpha)}(R)|^2, \quad (2)$$

where  $\chi_{\alpha'}^{(\alpha)}(R)$  represents the radial part of the relative wave function obtained by the CC calculation.  $\alpha$  represents the incident channel, which is the  $^8\text{Be}_{\text{g.s.}} + ^{16}\text{O}_{\text{g.s.}}$  channel in the present case, while  $\alpha'$  denotes the elastic or inelastic channel of the  $^8\text{Be} + ^{16}\text{O}$  system. The integration over  $R$  in Eq. (2) is cut off at  $R_{\max}$  because  $\chi_{\alpha'}^{(\alpha)}(R)$  is a scattering wave function.  $R_{\max}$  is chosen to be 7 fm, which is in vicinity of the barrier top of the relative potential between the colliding nuclei. The value  $I$  gives a measure of probability to find the system in the relevant channel component inside the barrier region, and it will show peaks at on-resonance energies when  $I$  is considered as a function of energy.

The solid curve in Fig. 1(A) represents the evaluated  $I$  in which the summation runs over all the channels included in the CC calculation within the grazing angular momenta  $J$

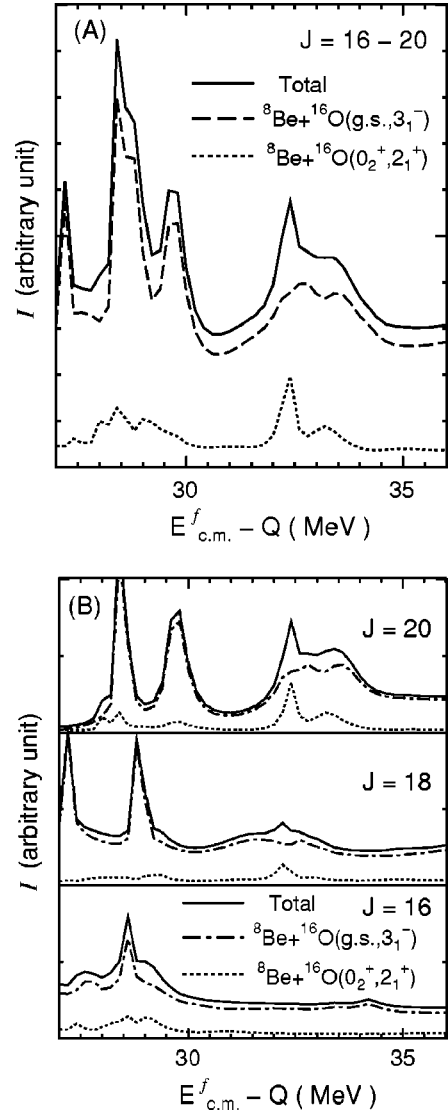


FIG. 1. Evaluated  $I$  defined by Eq. (2) for the  $^8\text{Be} + ^{16}\text{O}$  system as a function of energy. The solid curve represents the value summed over all the channels, and the dashed and dotted curves represent the components of the  $^8\text{Be}(g.s., 2_1^+, 4_1^+) + ^{16}\text{O}(g.s., 3_1^-)$  and the  $^8\text{Be}(g.s., 2_1^+, 4_1^+) + ^{16}\text{O}(0_2^+, 2_1^+)$  channels, respectively. The horizontal axis represents the center-of-mass energy of the incident  $^{12}\text{C} + ^{12}\text{C}$  system (see text for details). (A) The components of the grazing partial waves  $J=16-20$  are summed up. (B) The individual components of the grazing partial waves.

$=16-20$ . The horizontal axes of Fig. 1 represent the center-of-mass energy of the incident  $^{12}\text{C} + ^{12}\text{C}$  system, and hence the  $Q$  value ( $-0.205$  MeV) of the reaction is subtracted from the center-of-mass energy  $E_{\text{c.m.}}^f$  of the  $^8\text{Be} + ^{16}\text{O}$  system. It is found that the resonance peaks are obtained around 32.5 MeV and around 28.5 MeV where resonance peaks in the  $\alpha$ -transfer experiment were observed, when the evaluated  $I$  is shifted by about 3 MeV toward the low-energy side. One may think it a serious problem that the calculated excitation function has been shifted by 3 MeV to be compared with the experimental data. However, this amount of resonance-energy shift could be within a few percent uncertainty of the

nuclear-interaction model. One should note that only a few percent change of the strength of internuclear potential, obtained by the folding model, induces the same amount of shift of the resonance peaks. In fact, we have performed a CC calculation in which the strength of the  $N-N$  interaction is scaled, and found that a few percent scaling induces the shift of the resonance peaks by a few MeV, but the structures of  $I$  in Figs. 1(A) and 1(B) are not affected very much by the scaling. However, in the present paper, we use the same  $N-N$  interaction as that used in previous works [6,7] to avoid additional ambiguity due to the artificial change of the  $N-N$  interaction strength. Hereafter, all the calculated values are shifted by 3.0 MeV toward the low-energy side.

The dashed and dotted curves in Fig. 1(A) are the components of the  $^8\text{Be}(\text{g.s.}, 2_1^+, 4_1^+) + ^{16}\text{O}(\text{g.s.}, 3_1^-)$  and  $^8\text{Be}(\text{g.s.}, 2_1^+, 4_1^+) + ^{16}\text{O}(0_2^+, 2_1^+)$  channels, which have  $2\alpha + ^{16}\text{O}$  and  $2\alpha + (\alpha + ^{12}\text{C})$  configurations, respectively. It is clearly seen that the resonance peak around 32.5 MeV is due to the component of the latter channels, which have the  $2\alpha + (\alpha + ^{12}\text{C})$  four-cluster structure. From a detailed analysis of the wave function [12], it is found that this resonance is produced by the strong coupling among the rotational states in  $^8\text{Be}$  and among the  $0_2^+$  and  $2_1^+$  states in  $^{16}\text{O}$ . This means that the  $2\alpha + (\alpha + ^{12}\text{C})$  type four-cluster dynamics plays an essential role for generating the resonance, and that the resonance cannot be described by a single-channel resonance any longer. Since the  $(\alpha + ^{12}\text{C})$ -like excited states in  $^{16}\text{O}$  can easily be populated by the  $\alpha$ -transfer reaction, the resonance structure obtained in the present CC calculation in this channel could be a good candidate of the resonance observed in the  $\alpha$ -transfer reaction.

In Fig. 1(B), the values represented by the solid, dashed, and dotted curves in Fig. 1(A) are decomposed into each partial wave. It is found that the dominant spin of the peak at 32.5 MeV is  $J=20$ , and the  $J\leq 18$  waves also have non-negligible contribution. On the other hand, every partial wave shows a peak around 28.5 MeV, which is dominated by the  $2\alpha + ^{16}\text{O}$  channel component. A detailed discussion on the resonance properties in the  $^8\text{Be} + ^{16}\text{O}$  system will be reported in a forthcoming paper [12].

In order to confirm the relation between the resonances of the  $^8\text{Be} + ^{16}\text{O}$  system predicted by the above CC calculation and those observed in the  $\alpha$ -transfer reaction experiment, we perform a CCBA calculation using the distorted waves obtained by the CC calculations. For calculating the distorted waves of the  $^{12}\text{C} + ^{12}\text{C}$  system, we follow the procedure adopted by Ito *et al.* [6,7], except for neglecting the channels that are expected to play a minor role in the  $\alpha$ -transfer reaction. We include coupling among the ground state ( $0_1^+$ ) and the  $2_1^+$ ,  $3_1^-$ ,  $0_2^+$ , and  $2_2^+$  excited states. The latter two states are known to have a well-developed  $3\alpha$ -cluster structure. We use the transition densities among these states given by the  $3\alpha$  resonating-group-method (RGM) calculation [13]. A Woods-Saxon form imaginary potential, the parameters of which are taken from Refs. [6,7], is added to the folding-model potential. Consequently, the present CC calculation of the  $^{12}\text{C} + ^{12}\text{C}$  system shows almost the same results as those reported in Refs. [6,7].

TABLE I. The assumed oscillator quantum numbers of the intercluster motion for each state of  $^{12}\text{C}$  and  $^{16}\text{O}$ . Node ( $n$ ) and angular-momentum ( $\ell$ ) are listed with separation energy ( $E_s$ ) and spectroscopic factor ( $S$ ). The unit of  $E_s$  is MeV.

$^{12}\text{C}$	$n$	$\ell$	$E_s$	$S$	$^{16}\text{O}$	$n$	$\ell$	$E_s$	$S$
$0_1^+$	2	0	7.37	0.80	$0_1^+$	2	0	7.16	0.30
$2_1^+$	1	2	2.93	0.20	$0_2^+$	3	0	1.11	0.69
$0_2^+$	3	0	-0.29	1.80	$3_1^-$	1	3	1.03	0.30
					$2_1^+$	1	2	0.24	0.85

In terms of the CC wave functions calculated above, the CCBA  $T$ -matrix element for the  $\alpha$ -transfer reaction is written as

$$T_{\beta\alpha}^{\text{(CCBA)}} = \sum_{\beta'\alpha'} (S_{\beta'} S_{\alpha'})^{1/2} \times \langle \chi_{\beta'}^{(\beta)(-)}(\mathbf{R}') | F_{\beta'\alpha'}(\mathbf{R}', \mathbf{R}) | \chi_{\alpha'}^{(\alpha)(+)}(\mathbf{R}) \rangle, \quad (3)$$

where  $\alpha$  and  $\beta$  represent the entrance ( $^{12}\text{C}_{\text{g.s.}} + ^{12}\text{C}_{\text{g.s.}}$ ) and exit ( $^8\text{Be}_{\text{g.s.}} + ^{16}\text{O}_{\text{g.s.}}$ ) channels, respectively, and the summation runs over all the possible inelastic channels, denoted by  $\alpha'$  and  $\beta'$ , of the  $^{12}\text{C} + ^{12}\text{C}$  and  $^8\text{Be} + ^{16}\text{O}$  systems. Since the transfer processes via the mutual-excitation channels are higher-order processes, they are expected to have small contributions to the present  $\alpha$ -transfer reaction. Therefore, we only consider the  $\alpha$ -transfer processes through the following single-excitation channels,  $^{12}\text{C}_{\text{g.s.}} + ^{12}\text{C}(2_1^+)$ ,  $^{12}\text{C}_{\text{g.s.}} + ^{12}\text{C}(0_2^+)$ ,  $^8\text{Be}_{\text{g.s.}} + ^{16}\text{O}(0_2^+)$ ,  $^8\text{Be}_{\text{g.s.}} + ^{16}\text{O}(3_1^-)$ , and  $^8\text{Be}_{\text{g.s.}} + ^{16}\text{O}(2_1^+)$  in addition to the entrance ( $^{12}\text{C}_{\text{g.s.}} + ^{12}\text{C}_{\text{g.s.}}$ ) and exit ( $^8\text{Be}_{\text{g.s.}} + ^{16}\text{O}_{\text{g.s.}}$ ) channels, although all the mutual-excitation channels are included in the CC calculations to generate the distorted waves of these channels.  $F_{\beta'\alpha'}(\mathbf{R}', \mathbf{R})$  is the *finite-range* form factor calculated by the standard procedure in the *post-form* formalism [14,15]: the  $\alpha$ - $^8\text{Be}(\alpha$ - $^{12}\text{C})$  relative wave function in  $^{12}\text{C}$  ( $^{16}\text{O}$ ) used for the transfer form factor is given by the separation energy (SE) method, in which the potential geometry is assumed to be of Woods-Saxon type with a range parameter  $R = 1.25 A^{1/3}$  fm [ $A$  represents the mass of the core nucleus  $^8\text{Be}$  ( $^{12}\text{C}$ )] and a diffuseness parameter  $a = 0.65$  fm. The depth of the potential is adjusted to reproduce the separation energy, assuming the oscillator quantum number of the intercluster motion for each state listed in Table I. The potential generating the  $\alpha$ - $^8\text{Be}$  wave function is used as the interaction for  $\alpha$ -transfer reaction.  $S_{\alpha'}$  and  $S_{\beta'}$  represent the spectroscopic factors, which are evaluated from microscopic cluster-model wave functions [16–18] except for the  $3_1^-$  state of  $^{16}\text{O}$ . We assume the spectroscopic factor of the  $3_1^-$  state to be 0.30 which is the same as that of the ground state. The change of this value does not affect the essential feature of the resultant excitation function of the  $\alpha$ -transfer reaction. The values are also listed in Table I.

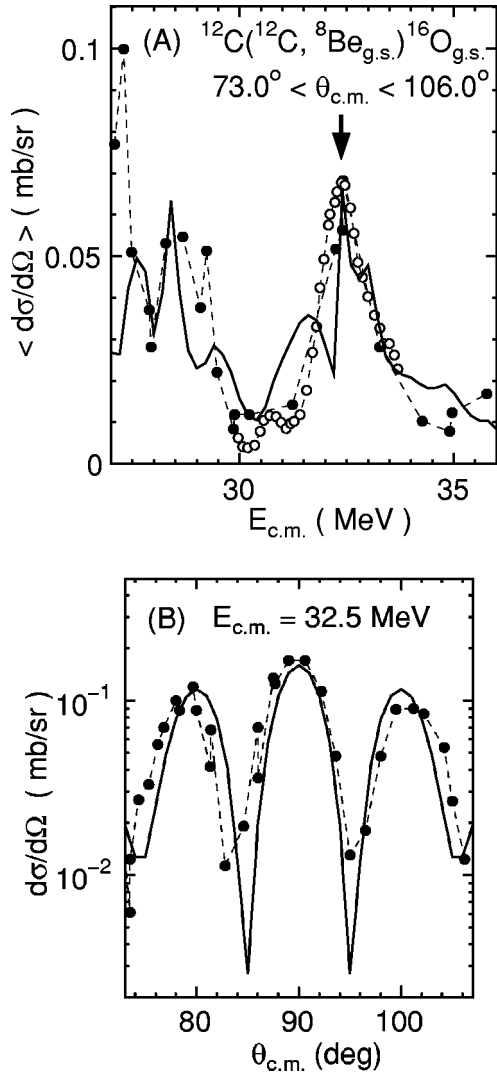


FIG. 2. (A) The energy dependence of the angle-averaged differential cross sections of the  $^{12}\text{C} + ^{12}\text{C} \rightarrow ^8\text{Be}_{g.s.} + ^{16}\text{O}_{g.s.}$  reaction. The open and filled circles with thin dashed curves are the experimental data [2–4], and the solid curve represents the result of the CCBA calculation. (B) The angular distribution around  $\theta_{c.m.} = 90^\circ$  at the on-resonance energy  $E_{c.m.} = 32.5$  MeV [indicated by an arrow in (A)]. The filled circles with thin dashed curve are the experimental data [2,3] and the solid curve represents the result of the CCBA calculation.

Figure 2(A) shows the energy dependence of the backward angle differential cross sections of the  $^{12}\text{C} + ^{12}\text{C} \rightarrow ^8\text{Be}_{g.s.} + ^{16}\text{O}_{g.s.}$  reaction averaged over the angular range  $\theta_{c.m.} = 73.0^\circ - 106.0^\circ$ . The open and filled circles are the experimental data [2–4]. The solid curve represents the result of the present CCBA calculation, which is shifted by 3.0 MeV toward the low-energy side and divided by a factor of 1.5 to be compared with the experimental data. The CCBA calculation reproduces well the characteristic behavior of the excitation function in this energy range. The characteristic enhancement of cross sections around  $\theta_{c.m.} = 90^\circ$  observed in the angular distribution at the on-resonance energy  $E_{c.m.} = 32.5$  MeV [indicated by an arrow in Fig. 2(A)] is also reproduced well, as shown in Fig. 2(B). The partial wave with

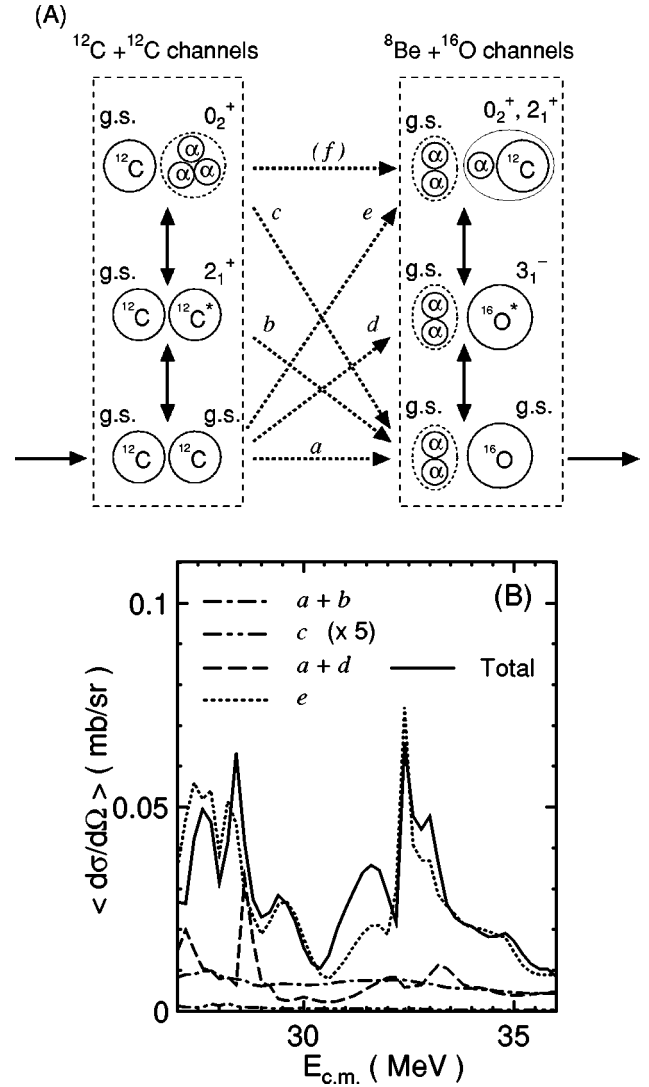


FIG. 3. (A) An illustration of the reaction paths included in the present analysis, and (B) the contributions of the paths. The dot-dashed, double-dot-dashed, dashed, and dotted curves in (B) show the contributions of the paths  $a+b$ ,  $c$ ,  $a+d$ , and  $e$ , respectively. The contribution of the path  $c$  is multiplied by a factor of 5 to be visible. The coherent sum of all the processes is shown by the solid curve, which is the same as that in Fig. 2(A).

a total angular momentum of  $J=20$  has a dominant contribution at this energy, although the other lower partial waves also have non-negligible contribution to produce the characteristic enhancement of cross sections around  $\theta_{c.m.} = 90^\circ$  shown in Fig. 2(B).

In order to find the reaction path that contributes most to this reaction in the resonance energy region, we have decomposed the cross section into the individual contributions of different reaction paths. In Fig. 3(A), the transfer reaction paths included in the present calculation are illustrated. The direct reaction path between the  $^{12}\text{C}_{g.s.} + ^{12}\text{C}_{g.s.}$  and  $^8\text{Be}_{g.s.} + ^{16}\text{O}_{g.s.}$  channels is labeled by  $a$ , while the paths through the  $^{12}\text{C}_{g.s.} + ^{12}\text{C}(2_1^+)$ ,  $^{12}\text{C}_{g.s.} + ^{12}\text{C}(0_2^+)$ ,  $^8\text{Be}_{g.s.} + ^{16}\text{O}(3_1^-)$ , and  $^8\text{Be}_{g.s.} + ^{16}\text{O}(0_2^+, 2_1^+)$  channels are labeled by  $b$ ,  $c$ ,  $d$ , and  $e$ , respectively, and the path through both the  $^{12}\text{C}_{g.s.}$

+  $^{12}\text{C}(0_2^+)$  and  $^8\text{Be}_{\text{g.s.}}+^{16}\text{O}(0_2^+)$  channels is labeled by  $f$ .

Figure 3(B) shows the contributions of the paths through  $a+b$ ,  $c$ ,  $a+d$ , and  $e$ , which are represented by the dot-dashed, double-dot-dashed, dashed and dotted curves, respectively. Since the  $^{12}\text{C}_{\text{g.s.}}+^{12}\text{C}_{\text{g.s.}}$  and  $^{12}\text{C}_{\text{g.s.}}+^{12}\text{C}(2_1^+)$  channels in the initial system have a  $^{12}\text{C}+^{12}\text{C}$  dinucleus type configuration, we sum up the contributions of the paths  $a$  and  $b$  coherently. Similarly, since the  $^8\text{Be}_{\text{g.s.}}+^{16}\text{O}_{\text{g.s.}}$  and  $^8\text{Be}_{\text{g.s.}}+^{16}\text{O}(3_1^-)$  channels in the final system have a  $2\alpha+^{16}\text{O}$  configuration, we sum up the  $a$  and  $d$  contributions coherently. The double-dot-dashed curve is multiplied by a factor of 5 to be visible. The coherent sum of all the processes is shown by the solid curve, which is the same as the solid curve in Fig. 2(A).

It is clearly seen that the process via the  $^8\text{Be}_{\text{g.s.}}+^{16}\text{O}(0_2^+, 2_1^+)$  channels has a dominant contribution in producing the resonance peak at  $E_{\text{c.m.}}=32.5$  MeV. These channels have a  $2\alpha+(\alpha+^{12}\text{C})$  four-cluster configuration, since the  $^{16}\text{O}(0_2^+, 2_1^+)$  states have a developed  $\alpha+^{12}\text{C}$  structure, as already mentioned. On the other hand, the processes via the  $^{12}\text{C}_{\text{g.s.}}+^{12}\text{C}(\text{g.s.}, 2_1^+)$  and  $^8\text{Be}_{\text{g.s.}}+^{16}\text{O}(\text{g.s.}, 3_1^-)$  channels have small contributions in this energy region, despite that they include the direct reaction path  $a$ . There is no prominent structure in the dashed curve, except for a sharp peak at 28.6 MeV. The contribution of the process via the  $^{12}\text{C}_{\text{g.s.}}+^{12}\text{C}(0_2^+)$  channel is almost negligible. It is also found that the reaction path through both the  $^{12}\text{C}_{\text{g.s.}}+^{12}\text{C}(0_2^+)$  and  $^8\text{Be}_{\text{g.s.}}+^{16}\text{O}(0_2^+)$  channels ( $f$ ) has a negligible contribution [though not shown in Fig. 3(B)].

Compared with Fig. 1, it is seen that the relative magnitude of the components of the  $2\alpha+^{16}\text{O}$  and  $2\alpha+(\alpha+^{12}\text{C})$  channels are inverted in Fig. 3(B). This is because the magnitude of the spectroscopic factor of the  $0_2^+$  and  $2_1^+$  states in  $^{16}\text{O}$  is larger than that of the ground and  $3_1^-$  states by a factor  $\sim 2.5$ . Another reason is the interference among the subchannels belonging to the respective group: destructively among the  $2\alpha+^{16}\text{O}$  channels, while constructively among the  $2\alpha+(\alpha+^{12}\text{C})$  channels. The result reported in this paper strongly suggests that the  $(\alpha+\alpha)+(\alpha+^{12}\text{C})$  type four-cluster states are populated in this reaction.

Finally, we mention the effect of the imaginary potential for the  $^8\text{Be}+^{16}\text{O}$  system, which is not considered in the present analysis. As mentioned above, the imaginary-potential parameters for the  $^8\text{Be}+^{16}\text{O}$  system cannot be determined phenomenologically. One of the simplest assumption would be to use the same imaginary potential for both the  $^{12}\text{C}+^{12}\text{C}$  and  $^8\text{Be}+^{16}\text{O}$  systems. We perform a test CCBA calculation using the same imaginary potential for both systems. In this calculation, a resonancelike structure also appears around  $E_{\text{c.m.}}=32.5$  MeV, and the characteristic feature that the process  $e$  via the  $2\alpha+(\alpha+^{12}\text{C})$  channels has a dominant contribution is unchanged. However, the absolute value becomes small, down to one-quarter the experimental data. This result suggests that the magnitude of the imaginary potential should be smaller for the  $^8\text{Be}+^{16}\text{O}$  system than that for the  $^{12}\text{C}+^{12}\text{C}$  system. One could find an optimum parameter set of the imaginary potential for the  $^8\text{Be}+^{16}\text{O}$  system that gives a better fit to the observed excitation function of the  $\alpha$ -transfer reaction. However, it makes the theoretical results less transparent, and hence we have switched off the imaginary potential for the  $^8\text{Be}+^{16}\text{O}$  system in the present analysis shown in Figs. 1–3.

In summary, we investigate the resonance structure observed in the  $^{12}\text{C}+^{12}\text{C}\rightarrow^8\text{Be}_{\text{g.s.}}+^{16}\text{O}_{\text{g.s.}}$  reaction around  $E_{\text{c.m.}}=32.5$  MeV by the method of CCBA. The experimental data of the excitation function as well as the angular distribution at the on-resonance energy are well reproduced by the calculation. From the result of the analysis, we conclude that the  $(\alpha+\alpha)+(\alpha+^{12}\text{C})$  type four-cluster states are populated in this  $\alpha$ -transfer reaction. It is very interesting to further study the  $\alpha$ -transfer reaction leading to the other exit channels, e.g.,  $^8\text{Be}_{\text{g.s.}}+^{16}\text{O}(0_2^+, 2_1^+)$ ,  $^8\text{Be}_{\text{g.s.}}+^{16}\text{O}(3_1^-)$  channels, and search for resonances in these channels, because they will provide a more direct test of the theoretical predictions of the present CC calculations.

One of the authors (M.T.) thanks the Japan Society for the Promotion of Science (JSPS) for financial support. This work was supported from JSPS by Grant-in-Aid for Scientific Research.

- 
- [1] A.H. Wuosmaa, R.R. Betts, B.B. Back, M. Freer, B.G. Glagola, Th. Happ, D.J. Henderson, P. Wilt, and I.G. Bearden, *Phys. Rev. Lett.* **68**, 1295 (1992).
- [2] M. Aliotta, S. Cherubini, E. Costanzo, M. Lattuada, S. Romano, D. Vinciguerra, and M. Zadro, *Z. Phys. A* **353**, 43 (1995).
- [3] M. Aliotta, S. Cherubini, E. Costanzo, M. Lattuada, S. Romano, C. Spitaleri, A. Tumino, D. Vinciguerra, and M. Zadro, *Z. Phys. A* **354**, 119 (1996).
- [4] R.A. Le Marechal, N.M. Clarke, M. Freer, B.R. Fulton, S.J. Hall, S.J. Hoad, G.R. Kelly, R.P. Ward, C.D. Jones, P. Lee, and D.L. Watson, *Phys. Rev. C* **55**, 1881 (1997).
- [5] Y. Hirabayashi, Y. Sakuragi, and Y. Abe, *Phys. Rev. Lett.* **74**, 4141 (1995).
- [6] M. Ito, Y. Sakuragi, and Y. Hirabayashi, *Few-Body Syst., Suppl.* **12**, 137 (2000).
- [7] M. Ito, Ph.D. thesis, Osaka City University, 2000.
- [8] A.M. Kobos, B.A. Brown, P.E. Hodgson, G.R. Satchler, and A. Budzanowski, *Nucl. Phys.* **A384**, 65 (1982).
- [9] M. El-Azab Farid and G.R. Satchler, *Nucl. Phys.* **A438**, 525 (1985).
- [10] M. Katsuma, Y. Sakuragi, S. Okabe, and Y. Kondō, *Prog. Theor. Phys.* **107**, 377 (2002).
- [11] S. Okabe (unpublished).
- [12] M. Takashina, M. Ito, and Y. Sakuragi, Ph.D. thesis, Osaka City University, 2003.
- [13] M. Kamimura, *Nucl. Phys.* **A351**, 456 (1981).
- [14] E. Mathiak, K.A. Eberhard, J.G. Cramer, H.H. Rossner, J.

- Stettmeier, and A. Weidinger, Nucl. Phys. **A259**, 129 (1976).
- [15] R.M. DeVries, Nucl. Phys. **A212**, 207 (1973).
- [16] Y. Fukushima and M. Kamimura, in *Proceedings of the International Conference on Nuclear Structure*, edited by T. Marumori [J. Phys. Soc. Jpn. Suppl. **44**, 225 (1978)].
- [17] Y. Fujiwara, H. Horiuchi, K. Ikeda, M. Kamimura, K. Katō, Y. Suzuki, and E. Uegaki, Prog. Theor. Phys. Suppl. **68**, 29 (1980).
- [18] S. Okabe, in *Tours Symposium on Nuclear Physics II*, edited by H. Utsunomiya *et al.* (World Scientific, Singapore, 1995), p. 112.